Physica Scripta. Vol. 32, 327–333, 1985.

Monte Carlo Simulations of the Quantum XXZ Model in Two Dimensions

53

E. Loh, Jr. and D. J. Scalapino

Department of Physics, University of California, Santa Barbara, California 93106, USA

P. M. Grant

IBM Research Laboratory, San Jose, California 95193, USA

Received 85-03-20 Accepted 85-04-02

Abstract

The XXZ spin Hamiltonian $H = -\sum_{\langle i,j\rangle} (S_i^x S_j^x + S_i^y S_j^y + \lambda S_i^z S_j^z)$ is simulated for quantum spins. The XY model ($\lambda = 0$) has a Kosterlitz-Thouless phase transition at $T_{KT} = 0.45 \pm 0.05$, slightly above which the specific heat has a finite peak. The vortex density has a non-zero value in the low-temperature limit, probably due to quantum fluctuations. The critical temperature holds up at least to $\lambda = -0.8$. The Ising transition temperature T_{Ising} is measured for Ising-like antiferromagnets $\lambda < -1$ and is found to drop off to zero in a manner consistent with the reciprocal-logarithmic behavior $T_c \propto -1/\log|-\lambda - 1|$, as proposed for the classical model.

1. Introduction

A variety of motivations exist for studying the XXZ Hamiltonian

$$H = -\sum_{\langle i,j\rangle} (S_i^x S_j^x + S_i^y S_j^y + \lambda S_i^z S_j^z) \tag{1}$$

in two dimensions. The first is, of course, the desire to model essentially two-dimensional magnetic materials. De Jongh and Miedema [1] review the basic magnetic properties of a number of such compounds. They find quite a few of these to be $s = \frac{1}{2}$ and on square lattices. Further, the ratio of the interplane coupling to the intraplane coupling is typically quite small – on the order of 10^{-6}.

The XXZ model may also be used as a lattice-gas model for two-dimensional fluids [2, 3]. Imagine a quantum lattice gas of hard-core bosons. Notice, incidentally, that the use of a lattice is not necessarily an artificial construction designed to represent a continuum. Indeed, in solid-state physics, lattices are usually the more physical situation (as in the case of a film adsorbed on a periodic substrate such as Grafoil). Allowing the bosons to hop from a site to any of the nearest neighbors gives

$$K.E. = -\sum_{\langle i,j\rangle} (\psi_i^\dagger \psi_j + \psi_j^\dagger \psi_i). \tag{2}$$

Interactions between bosons may be modeled by the term

$$P.E. \equiv \sum V(\mathbf{r}_i - \mathbf{r}_j) \to \sum_{\langle i,j\rangle} V_{ij} n_i n_j. \tag{3}$$

For our purposes, it will be sufficient to include only nearest-neighbor terms in this sum, corresponding to short-range interactions. Since we are only going to allow 0 or 1 bosons on each site, due to their hard cores, $\psi^2 = (\psi^\dagger)^2 = 0$. The two-state nature of the operators and the commutativity of bosons suggests a mapping onto spin-$\frac{1}{2}$ operators. Indeed, this was first done by Matsubara and Matsuda [2] who assigned $\psi^\dagger \to S^+ = S^x + iS^y$ and $n = \psi^\dagger \psi \to S^z + \frac{1}{2}$ recovering the XXZ Hamiltonian. Here the XY interaction plays the part of the kinetic energy, the ZZ interaction is the potential, and a magnetic field in the z direction corresponds to the chemical potential. Thus, the spin-$\frac{1}{2}$ XXZ model can be thought of as either an array of spins or as a fluid and the languages of the two models are often used interchangeably.

The spin-$\frac{1}{2}$ XXZ model happens also to be a strong-coupling approximation to an electron-exciton model which arises in the study of excitonic superconductivity [4]. Here, the model consists of a two-dimensional system of fermions, with spin-up and spin-down electrons wich are allowed to hop between nearest-neighbor sites, and there is a strong on-site attraction between particles. In the strong-coupling limit, spin-up electrons and spin-down electrons will want to sit upon the same sites. Hence, in the ground state, some fraction of the sites will be empty while the others will be fully occupied with an up-down pair. The fraction will of course depend on the density of electrons. In this limit, the ground state is highly degenerate – the energy being independent of the configuration of the pairs. The mapping of the Hubbard model to quantum spins is through the usual transformation $n_i \to S_i^z + \frac{1}{2}$. Since pairs are allowed to hop from site to site in this model, the spin Hamiltonian will include a term

$$-J_{xy} \sum_{\langle i,j\rangle} (S_i^+ S_j^- + S_i^- S_j^+) = -\frac{J_{xy}}{2} \sum_{\langle i,j\rangle} (S_i^x S_j^x + S_i^y S_j^y).$$

The degeneracy of the Hamiltonian with respect to the way the pairs are placed upon the lattice is lifted to second order in the hopping term of the Hamiltonian. For example, if a pair sits next to a vacancy, one member of the pair may hop virtually to the neighboring site and back again, lowering the energy of this isolated pair. If, on the other hand, that site is occupied, then this hopping process is blocked. Hence, pairs do not like to occupy neighboring sites, giving rise to an antiferromagnetic term in the spin Hamiltonian of the form $J_z \sum_{\langle i,j\rangle} S_i^z S_j^z$. Furthermore, the relevant matrix elements and energy denominators are such that $J_z > J_{xy}$ so that the resulting Hamiltonian will always be an Ising-like antiferromagnet [4].

Finally, a study of the XXZ model is of interest in the general theory of phase transitions since, by varying λ, the Hamiltonian can be made to exhibit behaviors of various universality classes. Consider, for example, the classical limit of the spin Hamiltonian

$$H = -\sum_{\langle i,j\rangle} \mathbf{S}_i \cdot \mathbf{S}_j, \tag{4}$$

where the $\mathbf{S}$ are n-component vectors of unit magnitude and the sum is over nearest neighbors. In two dimensions, n plays a crucial role. When $n = 1$, for example, the model becomes the two-dimensional Ising model, which Onsager has shown to have a phase transition at a finite temperature [5, 6]. Meanwhile, if $n \geqslant 3$ the spins fail to achieve long-range order at any finite temperature. The intermediate case, $n = 2$, also lacks long-range order [7]. Yet Stanley and Kaplan [8] concluded from high-temperature series expansions that the system underwent a phase transition in which the susceptibility diverged.

This 'paradox' was resolved by Kosterlitz and Thouless [9] by introducing topological long-range order, a low-temperature phase in which vortices are bound to antivortices. The phase is characterized by algebraic decay of the spin-spin correlation functions, as opposed to the exponential decays typical of high temperatures. As the temperature is increased more and more bound pairs are formed until, finally, at the critical temperature T_c, the pairs are allowed to 'boil' apart allowing free vortices. The two-dimensional XY model also exhibits a sharp peak in the specific peak just above T_c [10, 11]. Our XXZ model is rich in phenomenology, exhibiting behaviors that are characteristic of these different universality classes: $n = 1$ ($|\lambda| \geqslant 1$), $n = 2$ ($|\lambda| \leqslant 1$), and $n = 3$ ($|\lambda| = 1$).

Unfortunately, little work has been done on the general XXZ model for quantum spins. After Kosterlitz and Thouless [9] described topological long-range order in 1973, much work was done to describe the phase in greater detail for classical planar spins. In particular, some numerical work [10, 11] was done to measure the critical temperature for this model and to check estimates of exponents. The specific heat was found to have a finite peak just above the transition.

As one moves from planar spins to classical 3-component spins, however, increasing the z-z coupling strength can eventually destroy the Kosterlitz-Thouless phase transition and lead to Ising order. At the isotropic point $H = -\Sigma S_i \cdot S_j$, there is no order at any finite temperature. Some predictions [12, 13, 14] and numerical results exist for characterizing the crossover behavior between these different phases. It is predicted [12, 14] that the transition temperatures for both the Ising and Kosterlitz-Thouless phases should disappear logarithmically with the antisotropy for nearly isotropic systems:

$$T_c \propto 1/\log|\lambda - 1|. \tag{5}$$

This behavior is consistent with, but not necessarily confirmed by, numerical work [15, 16] for both sorts of anisotropy. It is worth noting that the very low-temperature behavior of the slightly Ising-like systems is not consistent with spin-wave theory [17] indicating the need either to include more complicated objects in the theoretical calculations (such as instantons) or indicating problems with the numerical results. The classical XXZ model has also been simulated with an additional quartic term $\alpha\Sigma(S^z)^4$ as a model of a *supersolid*, having both Kosterlitz-Thouless and Ising order [18].

Much less is known about the corresponding quantum mechanical spin-$\frac{1}{2}$ problem. In particular, since it is expected that the quantum and classical Hamiltonians both belong to the same universality classes, the quantum system is often ignored. High-temperature series expansions have been found [19] for the anisotropic Heisenberg model. Most other work is for $\lambda = 0$ – the XY model. Rogiers, *et al.* [20] used high temperature series expansions to estimate critical temperatures and exponents in this case. Both Pearson [21] and Suzuki and Miyashita [22] have variational estimates of the ground-state energy. Extrapolations from finite-size lattices also provide approximate values for the ground-state energy in addition to other quantities such as the susceptibility, vortex density, energy, specific heat, and entropy [23, 24, 25]. On the basis of such calculations, attempts have been made to characterize the ground state and the phase transition in the quantum XY model. A wide variety of real-space renormalization group approaches, characterized by uncontrolled approximations, have also been applied to this problem [26]. Unfortunately, they have been both inconclusive and contradictory. Finally, Monte-Carlo results exist for this model. This work is based on factoring the partition function trace $(e^{-\beta H})$ into many identical factors $(e^{-\Delta\tau H})^L$ where $\beta = L \cdot \Delta\tau$ and $\Delta\tau$ is taken to be small. No previous simulations exist for non-zero values of λ, but Suzuki, *et al.* [27] studied the case $\lambda = 0$ using very small values of $L (L = 1, 2)$, which casts doubt on the validity of their results at low temperatures (large β). De Raedt, *et al.* [28] studied the $L = 1$ model both analytically and by simulation and they simulated systems up to $L = 8$ as well. They found a divergent in-plane structure factor but a small out-of-plane susceptibility. In addition, several critical exponents were measured. Among their results, however, are the surprising – and we believe incorrect – conclusions that the specific heat diverges, in contrast with the classical-spin model [10, 11] and that the vortex density vanishes at zero temperature, as opposed to a finite value due to zero-point fluctuations suggested by exact small-lattice extra-polations [23].

In this paper, the quantum XXZ model is simulated for different values of λ. In section 2, the simulation technique is described. Section 3 reports results and a summary is given in section 4.

2. Simulation techniques

Direct applications of Monte Carlo techniques to qunatum mechanical systems are not possible since the matrix elements $\langle\psi|e^{-\beta H}|\psi\rangle$ are in general difficult, if not impossible, to evaluate. In the early sixties, Handscomb [29, 30] proposed that one write the partition function trace as a power series in βH. Since traces of powers of H are sometimes easily evaluated, his method had useful applications to several interesting quantum mechanical problems, including the isotropic Heisenberg ferromagnet [30] and, more recently, antiferromagnets as well [31]. The overwhelming majority of applicable techniques, however, centers around a path-integral representation of the partition function. Such algorithms [27, 32, 33, 34, 35, 36] typically expand the exponential as a product of many identical factors and then use the Trotter formula to approximate the essential matrix elements. The net effect of this expansion is to introduce an imagninary time, mapping a d-dimensional quantum mechanical problem into a $(d+1)$-dimensional classical one.

Let us start, then, by writing the path-integral representation of the partition function trace:

$$Z = Tr\, e^{-\beta H} = \sum_{\psi_i} \langle\psi_L|e^{-\Delta\tau H}|\psi_1\rangle\langle\psi_1|e^{-\Delta\tau H}|\psi_2\rangle \cdots \langle\psi_{L-1}|e^{-\Delta\tau H}|\psi_L\rangle, \tag{6}$$

where $\beta = L \cdot \Delta\tau$, the trace has been written out explicitly as a sum, and complete sets of states have been inserted between all adjacent exponentials. This expression for the partition function involves sums over L different d-dimensional states and so has incorporated the new imaginary-time dimension. We must now evaluate the matrix elements of the factors $e^{-\Delta\tau H}$. For sufficiently small values of $\Delta\tau$, one may approximate

$$e^{-\Delta\tau H} \approx e^{-\Delta\tau H_1} e^{-\Delta\tau H_2} \ldots e^{-\Delta\tau H_m} \tag{7}$$

where $H = H_1 + H_2 + \ldots + H_m$. Suzuki [32] has labelled this approximation the generalized Trotter formula and shows that the approximation becomes increasingly better as $\Delta\tau \to 0$, as we certainly hope it would. The reason this relation is simply an approximation is that the terms $H_1, H_2, \ldots, H_m$ do not, in general, commute with each other. It is up to us to choose these subhamiltonians cleverly and several choices have been suggested in the literature [27, 33, 34].

The breakup we use here is the checkerboard decomposition [35, 37], which has been found to be useful for one-dimensional systems with short-range interactions. Write $\exp(-\Delta\tau H) \approx \exp(-\Delta\tau H_1)\exp(-\Delta\tau H_2)$ where

$$H = -\sum_{\langle i,j \rangle} (S_i^x S_j^x + S_i^y S_j^y + \lambda S_i^z S_j^z) = H_1 + H_2 . \tag{8}$$

Here, H_1 and H_2 are each composed of cell Hamiltonians, each cell involving only four sites. This breakup is pictured in Fig. 1. Snce both H_1 and H_2 are made up of terms which commute amongst themselves, their exponentials may be broken up into exponentials of the four-site subhamiltonians without further approximation. These exponentials may be broken up in block diagonal form, the largest blocks being exponentiated numerically. Thus, matrix elements of $\exp(-\beta H)$ may be evaluated simply by breaking up the exponential into imaginary-time slices. Time slices act alternately on the two sets of plaquettes. The picture, then, is one of a (2 + 1)-dimensional structure filled with cubes that connect certain plaquettes on one time slice with the corresponding ones on the next slice. While it is clearly difficult to display a three-dimensional nest of cubes on a two-dimensional piece of paper, Fig. 2 attempts to do just that. This new lattice is surprisingly sparse; only one quarter of its volume is occupied by cubes. Each site in the (2 + 1)-dimensional lattice belongs to two cubes, one corresponding to H_1 and the other corresponding to H_2.

The system is now described by a (2 + 1)-dimensional configuration of spins which gives the evolution of the plane of spins through imaginary time. The overall weight of a particular path (that is, a particular (2 + 1)-dimensional configuration) is simply the product of all the matrix elements corresponding to the various cubes. Unfortunately, the matrix elements are not all positive – or even real! – and consequently the product is not necessarily positive, though sometimes it is, due to certain conservation properties. In many cases, this difficulty can be overcome by picking the appropriate representation for the quantum spins. If one quantizes the spins along the z-direction, then all of the matrix elements for the XXZ Hamiltonian

$$H = -\Sigma(S^x S^x + S^y S^y + \lambda S^z S^z)$$

are real and non-negative. Alternatively, it is sometimes useful to quantize the spins in the x-direction (to measure the response to spin twists about the z-axis, as will be described later). This

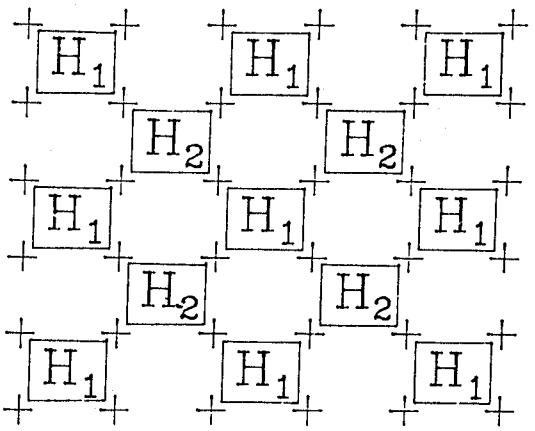

Fig. 1. Breakup of the two-dimensional lattice. The Hamiltonian is broken up into two pieces, H_1 and H_2. For each piece, the cell components commute amongst themselves.

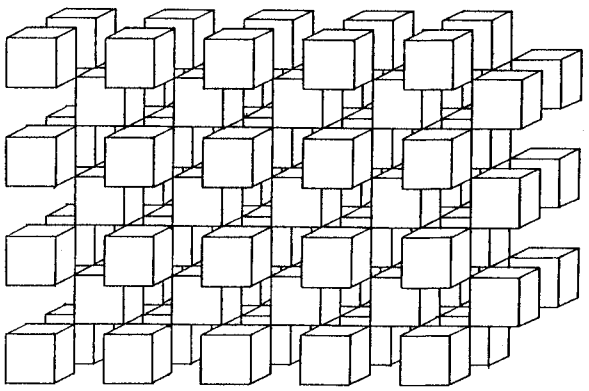

Fig. 2. (2 + 1)-dimensional lattice. Each site is a vertex for exactly two cubes. The space is one-quarter filled.

quantization gives exclusively non-negative matrix elements only for $|\lambda| < 1$, however, and has bad convergence properties as $|\lambda| \to 1$.

It is worth digressing for a moment to try to gain a feeling for what these imaginary-time paths mean. Let us take the z-quantization for now. If the spins actually represented hard-core bosons, as described earlier, we would say that we have chosen an occupation-number representation. The (2 + 1)-dimensional lattice, then, depicts the paths of some number of bosons in imaginary-time. The matrix element that corresponds to a given cube is nothing more than the many-particle propagator for bosons to evolve from one cube face to the face on the next time slice. It is helpful to assign world lines to the bosons and try to visualize them in (2 + 1)-dimensional space. Of course, the particles are actually indistinguishable, so that calculation of the matrix elements implicitly sums over all permutations among the particles and an unambiguous assignment of world lines to a configuration of occupation numbers is impossible.

Even if all matrix elements were non-negative, allowing us to interpret them as probabilities, it is important to realize that many of them can be zero. Indeed, it is impossible to get a new configuration with non-zero overall weight from an old one by flipping only one spin. The Monte-Carlo moves that are used to update the lattice, then, are four-site moves. Three moves are employed. One move takes a boson 'world line' from evolving via a given cube to evolving through its neighbor cube in the x direction. Similarly, one might grab a world line and 'pull' it in

the y direction. Such moves are analogous to those introduced by Hirsch *et al.* [37] for lattices with only one space dimension. Finally, there is a move which takes two adjacent lines which twist about each other and reassign them so that they twist in the opposite direction. These moves can be described more precisely by considering a 2×2 square of sites in the $(2+1)$-dimensional lattice which does not serve as a face for any cube. If this square is either in the x-τ plane or in the y-τ plane, then the move takes a boson world line from one of its edges to the other. If, however, the plaquette lies in the x-y plane, then the world lines must be thought of as passing through the square, instead of evolving along its edges. If two world lines pass through opposite corners of the square, then the third Monte-Carlo move simply forces the lines to pass through the other two corners. This effectively interchanges the world lines.

These moves span only a part of the configuration space [38], so that the Monte-Carlo simulation is not fully ergodic. In particular, the winding number of the world lines as well as the total number (i.e., the total magnetization) of world lines themselves are conserved. These restrictions, however, are unimportant in the thermodynamic limit where we are accustomed to having micro-canonical, canonical, and grand-canonical ensembles produce the same results for physical quantities despite the fact that some quantity (such as magnetization) may be held fixed. Marcu and Wiesler [39] have studied this question for quantum Monte-Carlo simulation in one dimension.

A large, but limited, number of observables may be measured by this approach. To be measurable, an operator must either have zero matrix elements if and only if the exponential of the cell subhamiltonian does, or, it must be a product of such operators. If the spins are quantized in the z-direction, therefore, it is possible to measure energy, specific heat, vortex density, vortex correlation, and $\langle S^z S^z \rangle$ correlations, as well as the dependence of these correlation functions on imaginary time τ.

The problem was run on an IBM 3081 computer with $\Delta\tau$ usually set to 0.25. Dependence of measurements on $\Delta\tau$ was tested and found to be quite small. Measurements were made 15,000 times with 2 sweeps of the lattice between measurements. Ten such runs were used to generate each point along with its error bar. Thus, each point represents $10 \times 15{,}000 \times 2 = 300{,}000$ sweeps of the lattice. Runs on lattices as large as $24 \times 24 = 576$ sites were performed, in contrast with exact diagonalizations, which stop around 18 sites. In the τ direction, we have used as many as $L = 40$ slices (for $T = 0.1$ with $\Delta\tau = 0.25$). Suzuki's work used only $L = 1$ and 2. Generating measurements of the desired observables at $T = 0.5$ ($L = 8$) for a 16×16 lattice with a prescribed set of boundary conditions takes just over three hours.

3. Results

3.1 *XY Model*

Quantizing the spins along the z-axis allows a large number of measurements to be performed. The energy per site is plotted in Fig. 3 for $\lambda = 0$, with error bars much smaller than the width of the lines. At high temperatures, our data fit closely to the high-temperature form $E\alpha - 1/4T$. At low temperatures, $E \to -0.543 \pm 0.002$ which agrees with estimates from both variational and exact diagonalization calculations. The statistical

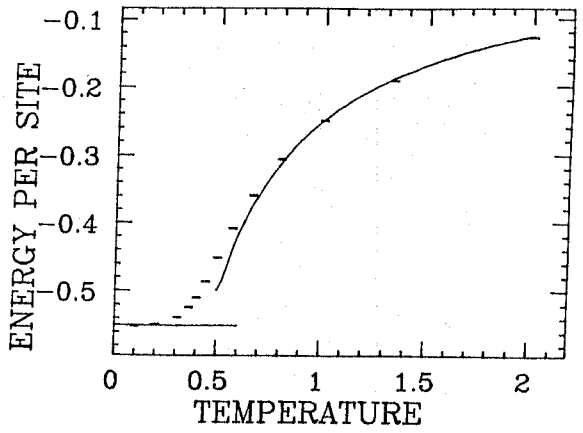

Fig. 3. Energy per site as a function of temperature for an 8×8 lattice of quantum spins with $\lambda = 0$. Results for the ground-state energy and a simple high-temperature expansion are shown for comparison.

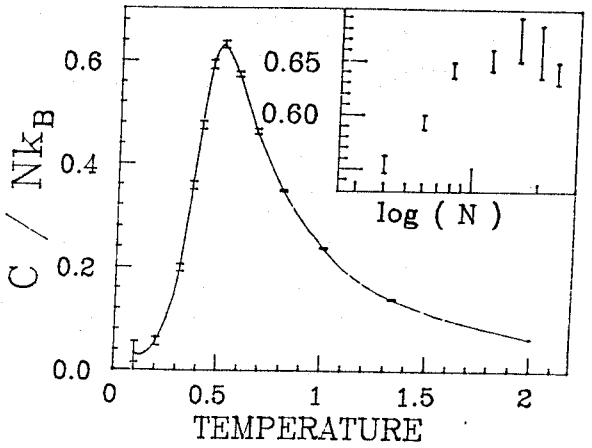

Fig. 4. Specific heat per site as a function of temperatur for 4×4 and 8×8 lattices of quantum spins with $\lambda = 0$. Points are found directly by measuring fluctuatings in energy. The inset shows the dependence of the peak height on size for 4×4 through 24×24 lattices.

error in our calculations is much smaller (10^{-4}). The quoted error is due to extrapolations in $\Delta\tau$, β, and lattice size.

In Fig. 4, the specific heat per spin, computed by measuring fluctuations in the energy, is shown for an 8×8 lattice, again with $\lambda = 0$. Numerical differentiation of the energy curve produces the same results. The specific heat peak occurs at $T = 0.5$. To test the dependence of this peak on lattice size, measurements were repeated on different lattices. The peak height clearly saturates in the thermodynamic limit at about $C/Nk_B = 0.65$, as shown in the inset. This is in contrast to the work of deRaedt *et al.* [28] who suggested a logarithmic divergence of the specific heat peak. Such a divergence would seem surprising, however, in light of the fact that the peak height does not diverge even in the classical-spin limit.

Since we expect the phase transition in this system to be driven by the unbinding of vortex pairs, it would be of interest to study the vortex density as a function of temperature. The vortex-density operator used here is Swendsen's [40] operator

$$V(T) = \frac{1}{4} \sum_{\text{plaquettes}} (1 - \sigma_1^x \sigma_3^x - \sigma_1^y \sigma_3^y)(1 - \sigma_2^x \sigma_4^x - \sigma_2^y \sigma_4^y), \tag{9}$$

where σ^x and σ^y are the x and y Pauli spin matrices. The sum is over all plaquettes and the subscripts refer to sites on the

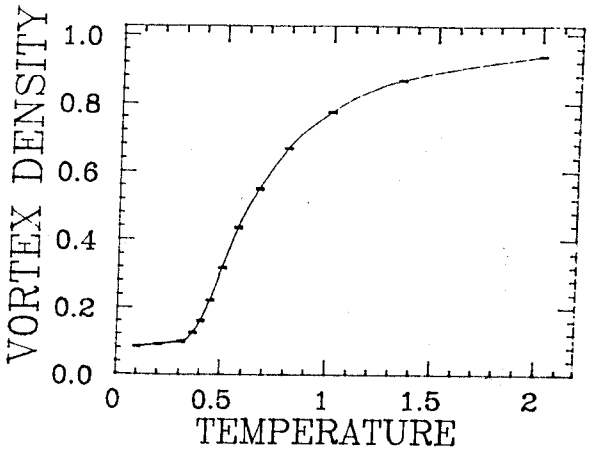

Fig. 5. Swendson's vortex density for quantum spins versus temperature for $\lambda = 0$. The vortex density is non-zero at $T = 0$ and exhibits a noticeable increase just below the critical temperature.

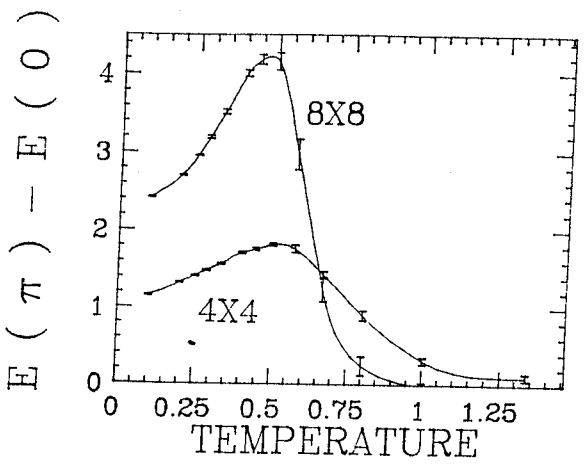

Fig. 6. Increase in the total internal energy due to a phase twist of π on a quantum system at $\lambda = 0$. Since this quantity is proportional to the derivative of the helicity modulus, the spike signals a Kosterlitz-Thouless phase transition.

vertices of each plaquette numbered in sequential order as one circles around. The vortex density is plotted in Fig. 5. It comes in to a non-zero value at $T = 0$, which qualitatively agrees with previous exact-diagonalization extrapolations and is to be expected from quantum zero point fluctuations. It is worth noting that $V(T)$ begins to grow noticeably at $T = 0.35 - 0.40$, which is just below where we estimate the phase transition to occur.

The helicity modulus γ has been proposed as a useful quantity for investigating Kosterlitz-Thouless phase transitions in the classical two-dimensional problem [41] and has been used successfully for this purpose in numerical studies [11]. For a spin system, the modulus is proportional to the spin-wave stiffness and characterizes the change in the free energy when a slow, in-plane, twist of the spins is made. In models of two-dimensional systems of bosons, it is proportional to the superfluid density. In the classical spin system, the modulus has a universal jump at the critical temperature [42]. Thus, we expect that the temperature-derivative of γ should provide a clear signal of T_c. Fortunately, this derivative is easy to measure since it is no more than the increase in the internal energy due to a twist.

If a phase twist is forced across the system – so that one edge of the system is held at $\vartheta = 0$ while the other end is held at $\vartheta = \Phi$ – then the resultant phase gradient $\varphi = \Phi/N_x$ results in an increase in the free energy

$$\frac{\Delta F}{N} = \frac{1}{2}\gamma|\varphi|^2 \tag{10}$$

for small phase gradients, where γ is th helicity modulus, N_x is the width of the system, and $N = N_x N_y$ is the total size of the system. Since, in Monte-Carlo simulations, one measures the total internal energy instead of the free energy, the increase in energy is related to the helicity modulus by

$$\Delta E \equiv \frac{\partial(\beta\Delta F)}{\partial\beta} = \frac{1}{2}\frac{\partial(\beta\gamma)}{\partial\beta}\varphi^2 \times N_x N_y. \tag{11}$$

When a phase twist of $\Phi = \pi$ is placed across the system in the x-direction, then $\varphi = \pi/N_x$, or,

$$\Delta E = \frac{\pi^2}{2}\cdot\frac{\partial(\beta\gamma)}{\partial\beta}\cdot\frac{N_y}{N_x} \tag{12}$$

Hence, the increase in the total internal energy due to a fixed twist is related to the derivative of the helicity modulus and should show a large spike at the transition temperature.

This energy increase is shown in Fig. 6 for 4×4 and 8×8 lattices of quantum spins with $\lambda = 0$. The phase twist has been forced on the system by quantizing spins along the x-axis, locking spins at $x = 0$ to lie along the $+x$ axis while the spins at $x = N_x$ are locked along the $-x$ axis. The peak of the energy increase occurs at $T = 0.45 \pm 0.05$, which gives us an estimate of the transition temperature, and is seen to increase with lattice size. Surprisingly, however, the helicity-modulus derivative increases with lattice size even far below the phase transition where size no longer plays a part in the classical-spin limit. The low-temperature limit of ΔE is plotted against lattice size in Fig. 7. This linear increase of ΔE with lattice wdith might be due to the formation of a domain wall. In this case, perhaps the phase twist π gets spread out over some length L rather than the entire lattice dimension N_x. Then,

$$\Delta E \propto \frac{1}{2}\frac{\partial(\beta\gamma)}{\partial\beta}\left(\frac{\pi}{L}\right)^2 L N_y \propto N_y, \tag{13}$$

resulting in a linear increase, as observed. If a domain wall is indeed forming, it is not clear whether that is an artifact of the

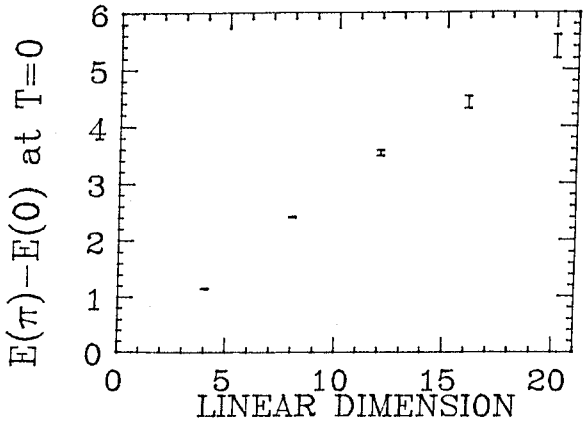

Fig. 7. Increase in the total internal energy due to a phase twist of π on quantum systems near $T = 0$ for $\lambda = 0$.

simulation technique or if it is a physical characteristic of the quantum system.

3.2 *XXZ Model*

In Fig. 8., the derivative of the helicity modulus is plotted for several different values of λ. The derivative peak occurs at the same temperature for all three values $\lambda = 0.0, -0.6, -0.8$, to within the accuracy of the calculations. This is consistent with results from the classical-spin model where the transition temperature does not drop off until very close to the isotropic case $\lambda = -1$. Unfortunately, it is difficult to explore the region for slightly XY-like Heisenberg systems because many matrix elements vanish, making successive Monte-Carlo configurations highly correlated.

Finally, the quantum XXZ model may be studied in the Ising regime $\lambda < -1$. Fig. 9 shows the staggered susceptibility of different sized lattices for $\lambda = -1.6$. The susceptibility appears to diverge independent of lattice size as the system is cooled but saturates at different size-dependent values as T drops below T_{Ising}. To get reliable estimates of the transition temperature, we have used a finite-size scaling analysis of the numerical data [43]. For an Ising transition, the correlation functions are known to drop off as $r^{-\eta}e^{-r/\xi}$ above T_{Ising} for large r, where η is the correlation-function exponent while ξ is the correlation length. In two dimensions, therefore, the suceptibility should go as

$$\chi \propto \int^{L} d^2 r r^{-\eta} e^{-r/\xi} = L^{2-\eta} g\left(\frac{L}{\xi}\right), \tag{14}$$

where L is the linear dimension of the system. Therefore, $\chi \cdot L^{\eta-2}$ should be a unique function $g(L/\xi)$ of L/ξ. Since $\eta = 0.25$ and $\xi \propto |T - T_{Ising}|^{-\nu}$ with $\nu = 1$ for the 2-d Ising model, the only parameter left to choose is T_{Ising}. The appropriate choice of T_{Ising}, of course, is the one which causes all plots of $\chi \cdot L^{\eta-2}$ against L/ξ to lie on top of each other for different lattice sizes L. Values of T_{Ising} calculated in this manner are plotted in Fig. 10 against $-1/\log(-\lambda - 1)$. The data appears to be consistent with predictions [12, 14] of this reciprocal logarithmic behavior for small anisotropy $(-\lambda - 1)$ for $(-\lambda - 1) < 0.5$. On the other hand, this reciprocal-logarithmic variation has dramatic behavior for only *very* small anisotropy $(-\lambda - 1) < 0.01$, suggesting that verification of this prediction must be investigated at values of λ much closer to -1.

4. Summary

The spin-$\frac{1}{2}$ XXZ model is expected to have the same universality classes as the classical model. At $\lambda = 0$, we find a Kosterlitz-Thouless transition at $T_{KT} = 0.45 \pm 0.05$ from helicity modulus measurements. We find the specific heat per site to have a peak just above T_{KT} whose height saturates at a finite value $C_{max}/Nk_B = 0.65$ with increasing lattice size. The finite specific heat peak height occuring at a temperature slightly greater than the transition temperature is characteristic of a Kosterlitz-Thouless transition. In contrast, previous simulation work on the quantum XY model suggested a logarithmic divergence of the specific-heat peak height. The vortex density, which is tied to the mechanism which drives the Kosterlitz-Thouless transition, rapidly starts to increase just below our estimate of the transition temperature. Its ground-state value appears to be non-zero due to quantum fluctuations in agreement with previous exact-diagonalizations but in disagreement with other simulation work.

We have performed the first simulations of the quantum model for $\lambda \neq 0$, locating the phase boundaries for several negative (antiferromagnetic) values of λ. The transition temperature seems to be nearly independent of the anisotropy for $0 \leqslant -\lambda \leqslant 0.8$. The system becomes Ising-like for $-\lambda > 1$. Our results are consistent with predictions of a reciprocal-logarithmic disappearance of the transition temperature with

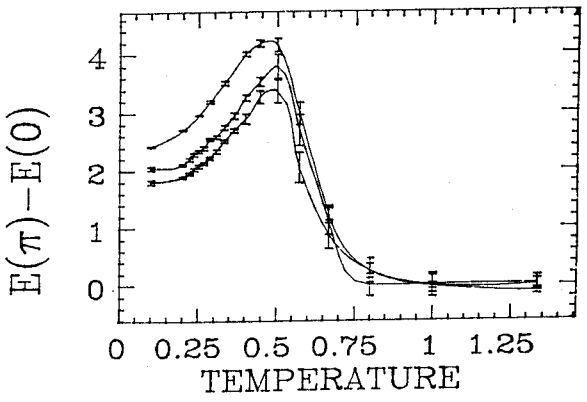

Fig. 8. Increase in the total internal energy due to a phase twist of π on quantum systems at $\lambda = 0.0, -0.6, -0.8$ measured on 8×8 lattices. All three peaks are essentially at the same place.

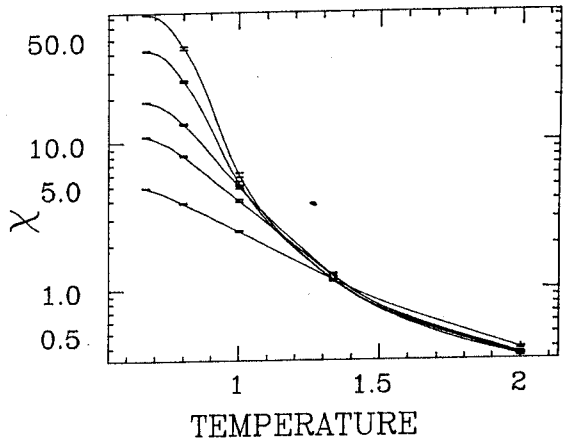

Fig. 9. Staggered out-of-plane susceptibility for the quantum XXZ model with $\lambda = -1.6$. Data is shown for 4×4, 6×6, 8×8, 12×12, and 16×16 lattices. Lines are drawn simply to guide the eye.

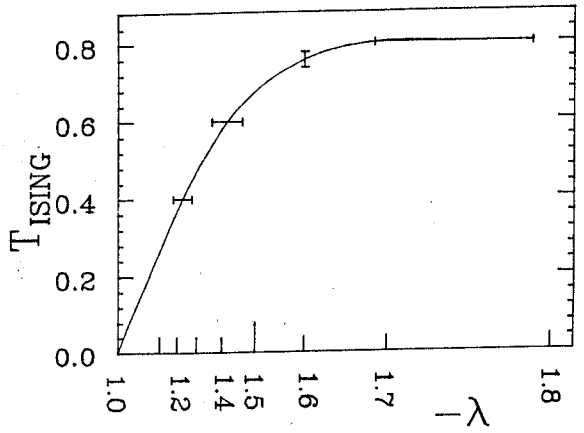

Fig. 10. Ising transition temperature T_{Ising} ploted against $-1/\log(-\lambda - 1)$. Work on the classical spin model predicts a straight-line behavior for $(-\lambda \approx 1)$.

anisotropy, although data taken much closer to $\lambda = -1$ is needed in order to make a more meaningful confirmation.

In addition to further simulation near the antiferromagnetic isotropic point, other interesting work remains to be done on the quantum XXZ model. There is room for much better algorithms as well as for a more complete understanding of the helicity-modulus. Even with the present algorithms, it should be possible to measure the modulus directly and also to produce better data for the ferromagnetic regime $\lambda > 0$. Finally, simulations of quantum Hamiltonians exhibiting supersolid phases – with both Kosterlitz-Thouless and Ising order – are of extreme interest. Such Hamiltonians could be understood as models of two-dimensional Bose films, the supersolid phases then corresponding to a solid with nonzero superfluid density. Supersolids have already been observed in simple classical spin models [18].

Acknowledgement

We would like to acknowledge Stig Lundqvist for his interest in and encouragement of our work on the simulation of quantum many-body systems. This work was supported in part by National Science Foundation Grant No. DMR83-20481. E. Loh, Nr. would also like to acknowledge receipt of partial financial support from an IBM Fellowship.

This work was supported in part by National Science Foundation Grant No. DMR83-20481. E. Loh would also like to acknowledge receipt of partial financial support from IBM.

References

1. de Jongh, L. J., and Miedema, A. R., Adv. in Phys. **23,** 1 (1974).
2. Matsubara, T., and Matsuda, K., Progr. Theoret. Phys. (Kyoto) **16,** 569 (1956) and **17,** 19 (1957).
3. Whitlock, R. T. and Zilsel, P. R., Phys. Rev. **131,** 2409 (1963).
4. Hirsch, J. E. and Scalapino, D. J., submitted for publication.
5. Onsager, L., Phys. Rev. **65,** 117 (1944).
6. Onsager, L. and Kaufman, B., Phys. Rev. **76,** 1232 & 1244 (1949).
7. Mermin, N. D. and Wagner, H., Phys. Rev. Lett. **22,** 1133 (1966).
8. Stanley, H. E. and Kaplan, T. A., Phys. Rev. Lett. **17,** 913 (1966).
9. Kosterlitz, J. M. and Thouless, D. J., J. Phys. **C6,** 1181 (1973).
10. Tobochnik, J. and Chester, G. V., Phys. Rev. **B20,** 3761 (1979).
11. Van Himbergen, J. E. and Chakravarty, S., Phys. Rev. **B23,** 359 (1981).
12. Dalton, N. W. and Wood, D. W., Proc. Phys. Soc. **90,** 459 (1967).
13. Pelcovitz, R. A. and Nelson, D. R., Phys. Lett. **57A,** 23 (1976).
14. Hikami, S. and Tsuneto, T., Progr. Theoret. Phys. **63,** 387 (1980).
15. Binder, K. and Landau, D. P., Phys. Rev. **B13,** 1140 (1976).
16. Kawabata, C. and Bishop, A. R., "Monte Carlo Simulation of the Two-Dimensional and Classical Heisenberg Model with Easy-Plane Anisotropy", preprint NSF-ITP-82-21 (1982).
17. Hohenberg, P., private communication.
18. Loh, E., jr., doctoral dissertation, University of California at Santa Barbara, 1985.
19. Jou, D. C. and Chen, H. H., J. Phys. **C6,** 2713 (1973) and other work quoted therein.
20. Rogiers, J., Grundke, E. W. and Betts, D. D., Can. J. Phys. **57,** 1719 (1979).
21. Pearson, R., Phys. Rev. **B16,** 11909 (1977).
22. Suzuki, M. and Miyashita, S., Can. J. Phys., **56,** 902 (1978).
23. Betts, D. D., Salevsky, F. C., and Rogiers, J., J. Phys. **A14,** 531 (1981).
24. Betts, D. D., and Kelland, S. B., J. Phys. Soc. Japan **52,** 11 (1983).
25. Kelland, S. B., unpublished. Quoted in Betts and Kelland (1983).
26. Tatsumi, T., Prog. Theor. Phys. **65,** 451 (1981); Takano, H. and Suzuki, M., J. Stat. Phys. **26,** 635 (1981); and others.
27. Suzuki, M., Miyashita, S. and Kuroda, A., Prog. Theor. Phys. **58,** 1377 (1977).
28. DeRaedt, H., DeRaedt, B. and Lagendijk, A., Z. Phys. **B57,** 209 (1984).
29. Handscomb, D. C., Proc. Cambridge Philos. Soc. **58,** 594 (1962).
30. Handscomb, D. C., Proc. Cambridge Philos. Soc. **60,** 115 (1964).
31. Lee, D. H., Joannopoulos, J. D. and Negele, J. W., Phys. Rev. **B30,** 1599 (1984).
32. Suzuki, M., Comm. Math. Phys. **51,** 183 (1976).
33. Suzuki, M., Miyashita, S., Kuroda, A. and Kawabata, C., Phys. Letters **60A,** 478 (1977).
34. DeRaedt, H. and Lagendijk, A., Phys. Rev. Lett. **46,** 77 (1981) and J. Stat. Phys. **27A,** 731 (1982); DeRaedt, H. and Lagendijk, A. Phys. Rev. **B27,** 921 (1983).
35. Hirsch, J. E., Scalapino, D. J., Sugar, R. L., and Blankenbecler, R., Phys. Rev. Lett. **47,** 1627 (1981); and Hirsch, J. E., Sugar, R. L., Scalapino, D. J. and Blankenbecler, R., Phys. Rev. **B26,** 5033 (1982).
36. Cullen, J. J. and Landau, D. P., Phys. Rev. **B27,** 297 (1983).
37. Barma, M. and Shastry, B. S., Phys. Rev. **B18,** 3351 (1978).
38. Sugar, R., informal conversations.
39. Marcu, M. and Wiesler, A. preprint THEP 83/6 of the Universitat Freiburg, December 1983.
40. Swendsen, R. H., Phys. Rev. Lett. **49,** 1302 (1982).
41. Fisher, M. E., Barber, M. N. and Jasnow, D., Phys. Rev. **A8,** 1111 (1973).
42. Nelson, D. R. and Kosterlitz, J. M., Phys. Rev. Lett. **39,** 1201 (1977).
43. Fisher, M. E. and Barber, M. N., Phys. Rev. Lett. **28,** 1516 (1972).